Journal of Colloid and Interface Science 436 (2014) 138–145

Contents lists available at ScienceDirect

Journal of Colloid and Interface Science

www.elsevier.com/locate/jcis

Cationic vesicles of a carnitine-derived single-tailed surfactant: Physicochemical characterization and evaluation of in vitro gene transfection efficiency

Trilochan Patra, Subhajit Ghosh, Joykrishna Dey *

Department of Chemistry, Indian Institute of Technology Kharagpur, Kharagpur 721302, India

ARTICLE INFO

Article history:
Received 25 June 2014
Accepted 23 August 2014
Available online 6 September 2014

Keywords:
Carnitine
Vesicle
Nanotubes
Microscopy
Gene transfection
Toxicity

ABSTRACT

Spontaneous vesicle formation in water by single-chain surfactants is rare. Here we show that in aqueous solution, a single-chain cationic surfactant 3-(dodecylcarbamoyl-2-hydroxypropyl)-trimethylammonium chloride (C_{12}-CAR) derived from D,L-carnitine spontaneously forms vesicles with hydrodynamic diameters in the range of 30–70 nm. A detailed self-assembly study of the C_{12}-CAR surfactant was performed for the first time by use of a combination of techniques, including surface tension, conductivity, fluorescence probe, dynamic light scattering and transmission electron microscopy. The cationic surfactant was found to have a reasonably low critical aggregation concentration (3.4 ± 0.2 mM) in water at 298 K. The vesicles were observed to be stable at the physiological temperature (310 K) over a long period of time. Although the vesicles formed were found to be unstable and exhibit vesicle-to-tubule transition in the presence of salt, in the presence of 10 mol% cholesterol the stability of vesicles is enhanced. When compared with lipofectamine-2000, the C_{12}-CAR was found to act as an effective gene transfection agent in COS-1 cell line. The surfactant-DNA complex was also found to be nontoxic toward CHO cells.

1. Introduction

Cationic liposomes-forming synthetic amphiphiles are relatively well established as carriers of DNA, antimicrobial, and anticancer agents [1,2]. Their applications have been found for all routes of drug delivery. They reduce toxicity of drugs in the target organ by modifying drug distribution and improve the therapeutic index observed with several antimony salts, [3] immunomodulators, [4] antifungal agents, [5] and antibiotics [6]. Presently, synthetic cationic liposomes of quaternary ammonium compounds that form stable and closed bilayers (vesicles) in aqueous solutions are used in gene delivery [7]. DNA and cationic vesicles form complexes that are prospective candidates for gene therapy. These non-viral carriers appear promising because of their simplicity, apparent lack of immunogenicity and inflammatory response, larger carrier capacity and higher fusogenic potential as compared with viral carriers [8]. The success of gene therapy is largely dependent on the development of gene delivery vectors. Synthetic vectors, such as cationic polymers and lipids interact with DNA through a highly cooperative process, leading to the condensation of the anionic polyelectrolyte. This co-condensation of oppositely charged polymers is a quasi-irreversible process leading to polydisperse microprecipitates containing hundreds of DNA molecules per particle. Complexes are heterogeneous with respect to their composition, size (50–500 nm), and shape (toroids, rods, and aggregates) [9]. These cationic multi-molecular aggregates are efficient for DNA delivery to cells in culture since their large size favors their contact with the cell surface by sedimentation, but severely restricts their biodistribution. This may explain the poor transfection efficiency of these complexes. In contrast to cationic polymers and lipids, cationic detergents interact with DNA reversibly [10]. This tendency has been observed experimentally for cationic detergents, such as cetyltrimethylammonium bromide (CTAB) [10]. The detergents are thought to destabilize the endosomal membrane and induce DNA release into the cytoplasm, in line with the good transfection efficiency observed with complexes of DNA bound to vesicles composed of neutral lipids and cationic detergents [11].

L-Carnitine is known to be a trimethylated amino acid (γ-trimethyl-β-hydroxybutyrobetaine) biosynthesized from the amino acids lysine and methionine. L-Carnitine acts as a cofactor required for fatty acid metabolism and energy production in human and animals [12]. It is found in high concentrations in muscles of both vertebrates and invertebrate animals. Carnitine is an extremely hydrophilic stable compound. It is non-toxic (rat oral LD50 > 5000 mg kg^{-1}), non-mutagenic and shows almost no skin

* Corresponding author. Fax: +91 3222 255303.
E-mail address: joydey@chem.iitkgp.ernet.in (J. Dey).

http://dx.doi.org/10.1016/j.jcis.2014.08.049
0021-9797/

irritation [12]. Therefore, carnitine is widely taken as a nutritional supplement. Carnitine and its derivatives are largely applied in cosmetics and in pharmacy. Carnitine has a positively charged quaternary amine group and β-hydroxy and α-carboxylic acid groups. The latter two moieties can be coupled to hydrophobic chains to produce a cationic surfactant. Several approaches for the synthesis of short alkyl chain and medium or long acyl chain carnitine esters have been reported in literature [13,14]. The long chain alkyl/acyl carnitine esters are also reported as potentially biodegradable cationic lipid for use in gene delivery, [14] and as antimicrobial agent [15]. Indeed, the strong surface activity as well as biocompatibility [16] allows them to be classified as "soft drugs" [17]. The poly(carnitine) derivative has also been suggested to be a new class of biomaterial for application in pharmacy, cosmetics and petrochemicals [12]. It has been reported that most of the single-chain acyl carnitine derivatives (zwitterionic surfactants) form micelles at low concentrations [18,19], whereas the double-chain diesters (cationic surfactants) of carnitine in dilute aqueous solution form flexible bilayers and vesicles [19,20]. The single-long-chain amide carnitine amphiphile having a chiral center as well as amide group and a hydroxyl group in the hydrocarbon tail can result in a strong intermolecular hydrogen-bonding (H-bonding) interaction in addition to the hydrophobic interactions. Thus, it was thought that such strong interactions among amphiphiles can promote bilayer formation even in the case of single-chain derivative. The objectives of the work are (i) synthesis of single-chain carnitine salt, 3-(dodecylcarbamoyl-2-hydroxypropyl)-trimethylammonium chloride (C_{12}-CAR) (see Fig. 1 for structure), (ii) study of interfacial properties in water, (iii) study of the self-assembly behavior of C_{12}-CAR in aqueous solution at lower and higher concentrations, (iv) in vitro evaluation of its potential applications in gene delivery, and (v) toxicity studies.

2. Experimental section

2.1. Materials

D,L-Carnitine hydrochloride was purchased from Sigma and 1-hydroxy benzotriazole (HOBt), dicyclohexylcarbodiimide (DCC), dodecylamine were from SRL, Mumbai, India, and were used without further purification. Analytical grade potassium chloride and sodium chloride were procured locally and were used as such. N-phenyl-1-naphthylamine (NPN), 1,6-diphenyl-1,3,5-hexatriene (DPH) and pyrene were purchased from Sigma–Aldrich (Bangalore, India) and were used after recrystallization from acetone–ethanol mixture. Cholesterol and 5(6)-carboxyfluorescein, CF (Aldrich) was used directly. The purity of the fluorescent probes was tested by the fluorescence emission and excitation spectra. All organic solvents were of good quality commercially available and were dried and distilled fresh before use. Aqueous solutions were prepared using doubly distilled water.

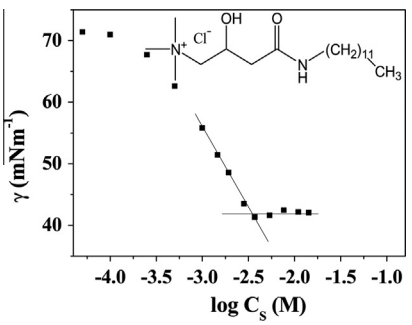

Fig. 1. Plot of γ vs. logC_S of C_{12}-CAR in water at 298 K; Inset: chemical structure of C_{12}-CAR.

Synthesis of C_{12}-CAR

The cationic surfactant C_{12}-CAR was synthesized following Scheme S1 (see "Electronic Supplementary Information", ESI) according to the procedure described elsewhere [21]. Briefly D,L-carnitine hydrochloride, (5.0 g, 0.0253 mol) was solubilized in DMF (150 mL) with stirring. Equimolar amounts of dodecylamine (4.69 g, 0.0253 mol) and DCC (5.22 g, 0.0253 mol) were dissolved in $CHCl_3$ (50 mL) separately and were poured into the stirring carnitine solution at room temperature. The reaction mixture was then cooled to about 5 °C in an ice bath. HOBt (3.42 g, 0.0253 mol) was dissolved in $CHCl_3$ (50 mL) and added drop wise to the above reaction mixture. After 1 h the reaction vessel was removed from the ice bath and stirring was continued for 24 h at room temperature. After completion of reaction, DMF was removed by vacuum distillation and the crude product was purified by column chromatography using silica gel (60–120 mesh) as the column packing material. Dry acetone was used to elute the impurities and acetone–methanol mixture (3:1 v/v) was used at the end to elute pure compound. Finally, the compound was recrystallized from dry acetone. The compound was identified by elemental analysis, FT-IR, and ^{1}H NMR spectra (Fig. S1, ESI).

C_{12}-CAR($C_{19}H_{41}O_2N_2Cl$). F.W.: 364.5. Yield 80%, M.P. 483 K (d), **FT-IR** (KBr, cm^{-1}): 3410, 3285, 2925, 2853, 1636, 1553, 1478, 1370, 1300. **^{1}H NMR**: Δ_H (200 MHz, D_2O): 4.57 (1H, m, C*H*), 3.41 (2H, *d*, *J* = 7.8 Hz, CH_2-CH), 3.16 (9H, s, NCH_3), 3.09 (2H, m, CH_2NH), 2.41 (2H, *d*, *J* = 6.2 Hz, CHCH_2CO), 1.43 (2H, m, $CH_2CH_2CH_2$), 1.19 (18H, m, alkyl chain), 0.73 (3H, *t*, *J* = 6.4 Hz, CH_3). **Elemental analysis** (CHNS/O) calcd. (%) 62.55, 11.25, 7.68 and found (%): 61.78, 11.44, 7.36.

2.2. Instrumentation and Methods

The ^{1}H NMR spectra were recorded on a Bruker SEM 200 MHz instrument in D_2O solvent using ACN as internal standard. The elemental analysis was carried out with a Perkin Elmer 2400 Series II CHNS/O analyzer. A Perkin–Elmer (Model Spectrum Rx I) spectrometer was used for recording the FT-IR spectra. For solid samples, KBr pellet was used, whereas in case of aqueous solutions (in D_2O), a thin layer of solution of the compound was placed between zinc selenide plates. The background spectrum of the pure solvent was then subtracted from the raw data using the instrumental software to obtain corrected spectrum. Melting points were determined by an Instind (Kolkata) melting point apparatus using open capillaries. Surface tension (ST) was measured in an automated Surface Tensiometer (model 3S, GBX, France) using the Du Nuöy ring detachment method. All measurements were performed at room temperature (~298 K) unless otherwise mentioned. Temperature controlled measurements were carried out by use of a temperature-controlled circulating water bath (JULABO, model F12).

A SPEX Fluorolog-3 (model no: FL3-11) spectrophotometer was used for recording fluorescence emission spectra of pyrene. A Perkin Elmer LS-55 luminescence spectrometer equipped with thermostating cell holder was used for steady-state fluorescence measurements with NPN and DPH probes. The steady-state fluorescence anisotropy (*r*) of DPH was measured on the Perkin Elmer LS-55 luminescence spectrometer. Fluorescence lifetimes (τ_f) of DPH probe were determined from time-resolved intensity decay by time-correlated single-photon counting method using a pico-second diode laser (λ = 370 nm, IBH, UK, nanoLED-03) as a source for excitation.

The dynamic light scattering (DLS) measurements were carried out with a Zetasizer Nano ZS (Malvern Instrument Lab, Malvern, U.K.) light scattering spectrometer equipped with a He–Ne laser

operated at 4 mW at λ_o = 633 nm, a digital correlator, and a computer-controlled and stepping-motor-driven variable angle detection system.

The high resolution transmission electron microscopic measurements were carried out on a HRTEM (JEOL-JEM 2100, Japan) operating at 200 kV at 298 K. A 400 mesh carbon-coated copper grid was immersed in a surfactant solution for 1 min, excess solution was blotted off with filter paper, air dried for an hour. It was then negatively stained with freshly prepared 1.5% (w/v) aqueous uranyl acetate. The specimens were kept in desiccators until before use.

For fluorescence microscopy, solid C_{12}-CAR surfactant (250 mM) was dissolved in a 1 mM aqueous solution of CF. The solution was equilibrated for about 4 h and then eluted through a Sephadex G-50 size exclusion column to remove the excess free dye from the dye-trapped aggregates. The diameter and height of the column were 1.2 cm and 25 cm, respectively. The eluent was collected and an aliquot of the sample solution was pipetted onto the glass slide and sealed with a cover slip and left to sit with the cover slip down for a few minutes before analysis. The confocal fluorescence microscopic images were obtained with a FV 1000 Olympus Confocal Microscope equipped with a laser scanning module (LSM) microscope and a PLAPON 60 X oil immersion objective with numerical aperture (NA) of 1.42.

3. Results and discussion

3.1. Critical micelle concentration

Studies on some long-chain acyl carnitines and perfluoroalkylacyl carnitines have shown high solubility, strong surface activity, and a significant emulsifying power of this single-chain carnitine surfactant. [16,18,19] Therefore, the aggregation behavior of the cationic surfactants C_{12}-CAR in aqueous medium was attempted first. The critical aggregation concentration (*cac*) of the surfactants was measured by the surface tension (ST) method. The surface tension (γ mN/m) was measured in water with increasing surfactant concentration (C_S) at 298 K. The γ value decreases linearly with logC_S (Fig. 1) and show a characteristic break and remains constant thereafter. The concentration corresponding to the break point was taken as *cac* value. The surface-active parameters, such as *cac*, surface tension corresponding to *cac* (γ_{cac}), and efficiency of adsorption, pC_{20} (negative logarithm of surfactant concentration required to reduce the ST of water by 20 units) were determined from the ST plot and the data are listed in Table 1.

The nature of the aggregates in aqueous solution can be further asserted by calculation of the values of the maximum surface excess concentration (Γ_{max}) and minimum surface area per surfactant head group (A_o) at the air/water interface. Γ_{max} was estimated from the slope of the linear part of the ST plot using Gibbs adsorption equations [22]

$$\Gamma_{max} = -1/nRT\ (d\gamma/d\ln C) \quad (1)$$

$$A_o = 1/(\Gamma_{max}\ N_A) \quad (2)$$

where the terms have their usual meanings. In Eq. (1) the value of n was assumed to be 2 as C_{12}-CAR is a 1:1 electrolyte. However, as discussed elsewhere, for some 1:1 cationics the n-value was found to be less than 2 because of the presence of ionic impurities [23]. However, in the present case, the feature of the adsorption isotherm clearly indicates absence of any surface-active impurity in the aqueous solution of C_{12}-CAR. The A_o value thus obtained from Eq. (2) using the Γ_{max} value is less than 100 Å^2 which is an indicative of the formation of bilayer aggregates [24]. It is well known that for a bilayer self-assembly, the hydrophobic chain modulates the phase behavior, whereas the head-group determines the bilayer surface chemistry. Intermolecular H-bonding among the head-groups and tight packing of the hydrocarbon tails in amphiphiles are responsible for the formation of spherical bilayer vesicles in dilute aqueous solution and has been reported earlier [25,26]. Similarly, in the case of C_{12}-CAR, the presence of amide and hydroxyl groups promotes intermolecular H-bonding, whereas the long hydrocarbon chain is responsible for the close packing of the molecules in bilayer formation, and has been supported by the results of fluorescence and microscopic studies discussed below.

3.2. Fluorescence probe studies

The fluorescence characteristics of polarity sensitive probes when bound to the hydrophobic domains give information on the nature of their microenvironments and hence the structure formation by the self-assemblies. It is well known that due to tight packing the hydrocarbon domain of the bilayer aggregates is much less polar than pure solvents [25,27]. The fluorescence spectra of two probes, pyrene and NPN were measured in the absence as well as in the presence of the surfactant to determine the polarity of the microenvironment of surfactant aggregates. Pyrene is a well-known polarity sensitive fluorescence probe, where the ratio (I_1/I_3) of intensities of the first and third vibronic bands of the pyrene fluorescence spectrum (Fig. S2(a) of ESI) is sensitive to the polarity of the microenvironment in which the probe is solubilized [28]. The I_1/I_3 ratio that has the highest value in water decreases with the decrease in solvent polarity. As surfactant molecules are mostly present in the aggregate form at a concentration equal to 10 mM (see Fig. 2), the I_1/I_3 ratio for C_{12}-CAR amphiphile was measured at this concentration. The I_1/I_3 ratio (Table 1) thus obtained was found to be much less than that of water (1.80), indicating solubilization of the pyrene molecule within the nonpolar microenvironment of the self-assembled microstructures [28]. In order to quantify the polarity of the hydrophobic microenvironment of the aggregates, I_1/I_3 value can be compared with the respective values of micelle-forming common cationic surfactants such as dodecyltrimethylammonium bromide (DTAB) having

Table 1
Surface-active parameters and self-assembly properties of C12-CAR at 298 K.

Properties	C_{12}-CAR
cac (mM)	3.4 ± 0.1
γ_{cac} (mN m^{-1})	41.5
pC_{20} (M)	2.8
$\Gamma_{max} \times 10^6$ (mol m^{-2})	2.4
A_o (Å^2 molecule^{-1})	70 ± 10
I_1/I_3[a]	1.27 ± 0.05
$\Delta\lambda_{NPN}$ (nm)[a]	20 ± 2
r[a]	0.125 ± 0.005
η_m (mPa s)[a]	34.0 ± 4

[a] Measured using [surfactant] equal to 10 mM.

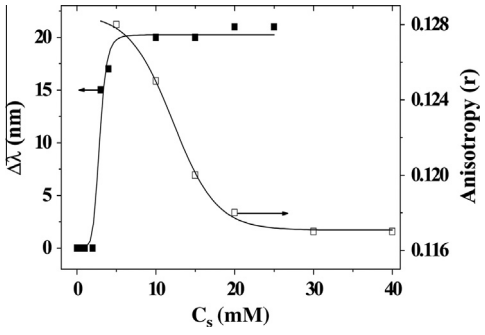

Fig. 2. Plots of variation of wavelength shift of NPN, $\Delta\lambda_{max}$ (=$\lambda_{water} - \lambda_{surfactant}$) and fluorescence anisotropy (r) of DPH vs. C_{12}-CAR concentration (C_S) at 298 K.

similar hydrocarbon chain length, neglecting the effect of counter ion on surfactant aggregate. It has been found that the microenvironment of the probe in C_{12}-CAR vesicles is less polar than that in DTAB micelles [29]. This suggests the existence of a more ordered and compact structure in C_{12}-CAR aggregates in comparison with DTAB micelles.

Also in the emission spectrum of NPN (Fig. S2 (b) of ESI) a shift in the emission maximum accompanied by a huge increase in fluorescence intensity relative to that in water was observed. This suggests solubilization of the probe within the rigid nonpolar microenvironment of the surfactant aggregates [30]. The variation of $\Delta\lambda_{max}$ with the surfactant concentration is shown in Fig. 2. The I_1/I_3 and $\Delta\lambda_{max}$ values of the corresponding probe measured in 10 mM surfactant solutions are listed in Table 1.

Similar to the change of fluorescence intensity of pyrene and NPN probe the fluorescence anisotropy (r) of DPH probe can also change when it is incorporated into the hydrophobic region of the surfactant aggregates [31]. The r-value (0.125 ± 0.002) of the DPH probe in the presence of C_{12}-CAR measured at a concentration above its *cac* value was found to be greater than that of DTAB (20 mM) micelles (r = 0.048), but is comparable to many vesicle- or liposome-forming amphiphiles [24,31]. The relatively high value of r suggests that the microenvironment of the probe molecule is very viscous [32]. This is possible only if bilayer structures are formed. In other words, r-value is sensitive to changes of microstructure of the self-assemblies. The r-value was also measured in the presence of different concentrations of C_{12}-CAR above *cac*. The plot (Fig. 2) shows that the r-value gradually decreases with the increase of surfactant concentration reaching minimum (0.117) at C_S equal to 40 mM. The small decrease of r-value can be attributed to the increase of light scattering by the vesicles the concentration of which increases with the addition of surfactant. This means that bilayer vesicles exist in a wide range of concentrations of C_{12}-CAR in aqueous solutions.

The above experimental findings can be further supported by the microviscosity (η_m) around the DPH probe, which gives a quantitative idea about the rigidity/viscosity of the microenvironments in the surfactant self-assemblies formed. The η_m value was obtained from the fluorescence lifetime (τ_f) and anisotropy data of DPH probe. A representative fluorescence intensity decay profile of DPH probe in 10 mM aqueous solution of C_{12}-CAR is shown in Fig. S3 of ESI. The τ_f value obtained from the analysis of fluorescence intensity decays of DPH probe in the presence of C_{12}-CAR surfactant is 4.35 ns. The η_m value around the probe molecule was calculated according to the procedure reported in a earlier publication [33]. The η_m values, thus calculated from the measured r and τ_f values of DPH probe (see Table 1) is much higher than those of normal micelles of cationic surfactants such as DTAB (13.22 mPa s) [33], indicating more rigid microenvironment in C_{12}-CAR vesicles. The magnitude of fluorescence lifetime and microviscosity sensed by the DPH probe solubilized in the self-assemblies of C_{12}-CAR is comparable to many liposome systems [24,31–34] and therefore, η_m value of C_{12}-CAR amphiphile is consistent with the formation of bilayer vesicles.

3.3. Molecular interactions responsible for the self-assembly formation

The supramolecular arrangement of C_{12}-CAR in the bilayer vesicle can be explained by the existence of hydrophilic/lipophilic, electrostatic, van der Waals and H-bonding interactions between the surfactant molecules. The first region on either side of the bilayer is the hydrophilic head-group formed by the quaternary ammonium group (Me_3N^+) of C_{12}-CAR and hence, this portion of the membrane is completely hydrated and facing toward the inner aqueous core of the vesicle. Next to the hydrated region is an intermediate region having polar hydroxyl and amide groups. It can be assumed that the —OH group present nearer to the Me_3N^+ group may be partially hydrated and involved in intermolecular H-bonding with neighboring molecules. In dilute solutions of the vesicles, the intermolecular H-bond formation between the OH-groups of C_{12}-CAR molecules must be mediated through interfacial water molecules and, therefore is relatively weaker than in concentrated solution of C_{12}-CAR. Therefore, FT-IR spectrum (Fig. S4) of the concentrated solution (20 mM) of C_{12}-CAR in D_2O solvent was taken to trace the existence of intermolecular H-bonding, and thus to provide a means of measuring the extra stability toward the aggregate formation in solution state. The FT-IR spectrum of C_{12}-CAR was recorded in D_2O solvent instead of H_2O because the O—H bond stretching in H_2O ($\sim$3360 cm^{-1}) and in the hydroxyl group ($\sim$3330 cm^{-1}) are very close, resulting in a band overlap. However, the O—D bond stretching and bending vibrations in D_2O appears at $\sim$2500 cm^{-1} and $\sim$1210 cm^{-1}, respectively. Also the H-bonding properties of the OH groups in D_2O do not differ greatly from that of the normal water (H_2O). Fig. S4 shows a broad peak around 3417 cm^{-1} corresponding to the O—H stretching frequency, suggesting intermolecular H-bonding between the —OH groups in the bilayer membrane. It should also be noted that DTAB surfactant with similar hydrocarbon chain length forms only micelles in aqueous solutions [35]. This means that —OH and the HNC=O functional groups in the hydrocarbon chain of C_{12}-CAR play a major role in the formation of bilayer aggregates.

Stable intermolecular H-bonding between N—H and C=O in the amide group of C_{12}-CAR that induces bilayer formation is also expected. In fact, similar H-bonding interaction has been reported for many vesicles-forming surfactants [36–38]. Existence of such interactions in the self-assembled structure of C_{12}-CAR is indicated by the low interfacial polarity reported by the NPN as well as by pyrene probe molecules (see data in Table 1). The low micropolarity suggests expulsion of water molecules from the interfacial region, reducing the possibility of formation of amide-water H-bonding and increasing the strength of amide-amide intermolecular H-bonding. These H-bonding interactions near the head-group region are able to minimize the repulsive interactions among the cationic Me_3N^+ groups thus ensuring higher stability to the bilayer membrane. The hydrophobic bilayer membrane of C_{12}-CAR composed of straight chain alkyl group (dodecyl) is also due to the strong hydrophobic interactions among the hydrocarbon chains. Thus based on the above results a schematic diagram of the bilayer structure (Fig. 3) formed by C_{12}-CAR surfactant can be proposed.

3.4. Hydrodynamic size of aggregates

The mean hydrodynamic diameter (d_H) of the surfactant aggregates was measured by the DLS technique at different concentrations. The size distribution histograms of the 5 mM and 20 mM C_{12}-CAR solutions are presented in Fig. 4. Both the distributions show the existence of mostly large aggregates along with some small aggregates (d_H = 3–4 nm) in equilibrium with large aggregates. The large aggregates have d_H in the range of 30–100 nm. The d_H values of these aggregates are observed to be very large in comparison with normal spherical micelles (3–5 nm) [39] of cationic surfactants. The large size of the aggregates is consistent with the vesicular structures as suggested by the results of fluorescence depolarization and ST measurements.

3.5. Shape of the aggregates

Microscopy

In order to visualize the shape, size and morphology of the microstructures formed by the surfactant in aqueous solution,

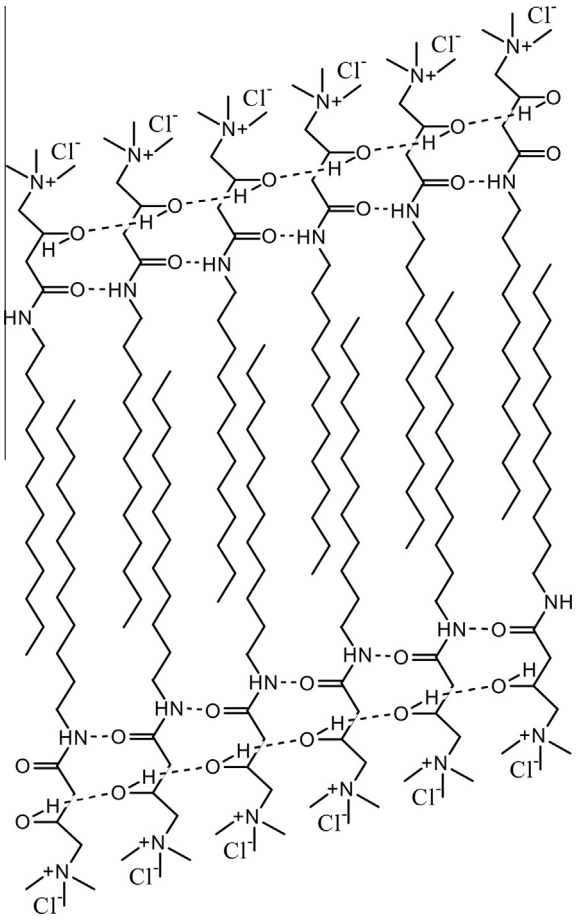

Fig. 3. Schematic diagram of the bilayer structure formed by C_{12}-CAR amphiphile in aqueous solution.

HRTEM images (Fig. 5) of C_{12}-CAR solutions were taken. The TEM images in Fig. 5(a) and (b) clearly exhibit the presence of almost spherical bilayer vesicles that enclose an aqueous cavity at both lower and higher concentrations. This finding is consistent with the results obtained from ST and fluorescence studies. It can be seen thInstrumentation and Methodsat the inner diameters of the vesicles are approximately in the range 30–70 nm which are slightly less than the mean hydrodynamic diameters obtained from DLS measurement. This might be due to the drying of the sample in TEM method.

Since the circular structure of the vesicles with aqueous interior usually observed in normal TEM micrographs is often criticized as artifacts due to the sample preparation procedure, the vesicle formation with enclosed aqueous cavity was further demonstrated by fluorescence microscopy (dye entrapment method). Incorporation of fluorescent dyes into the liposome and vesicle has been widely used for the study of stability, release profile, membrane fusion, and tracking of liposomes and vesicles [34]. In order to further support the existence of interior aqueous core and therefore, the existence of vesicles, fluorescence microscopy of a highly water-soluble fluorescent dye CF trapped vesicle solution of C_{12}-CAR was performed. The microscopic image in Fig. 6(a) exhibits its circular structures showing green fluorescence, clearly indicating entrapment of CF molecules within the aqueous core of the vesicles. However, only large size vesicles could be detected due to the limited resolution of the fluorescence microscope.

3.6. Effect of salt on vesicle stability

The effect of salt concentration on the stability of vesicles formed by C_{12}-CAR surfactant was systematically studied. It is commonly observed that increase of counter ion concentration or even an increase of ionic strength of the surfactant solution induces transition of bilayer vesicles to form spherical micelles [40], rod-like micelles [41], tubular structure [42] or from small vesicles to giant vesicles [43]. Addition of salts causes the reduction of electrostatic repulsion among the surfactant head-groups and is a key factor to influence the morphology of aggregates in ionic surfactant solutions [42]. Also addition of salts causes the reduction of *cac* value as the aggregation becomes more favorable due to the reduction of electrostatic repulsion among the surfactant head-groups. In the present case, the *cac* value is reduced to 0.71 mM in the presence 50 mM NaCl salt (see Fig. S5) at room temperature.

To understand the influence of salt concentration on surfactant aggregates, the steady-state fluorescence anisotropy (r) of DPH probe was measured in C_{12}-CAR solution at concentrations above its *cac* value in the presence of varying concentration of NaCl. The variation of r with [NaCl] is shown in Fig. 7(a). The plot shows a sharp decrease of r-value with the rise of NaCl concentration, suggesting transformation of bilayer structure to some other morphology at a relatively low NaCl concentration (~50 mM). Since r-value at the highest salt concentration used is not as low as that of normal micelles (~0.05), this is indicative of the transformation of vesicles-to-rod-like/tubular aggregates.

The DLS measurements using 5 mM C_{12}-CAR was also performed in the presence of 50 mM NaCl. The results are presented in the inset of Fig. 7(a). The mean d_H value is found to be around 1.0 μm, which is much higher than the value obtained in the absence of salt. This indicates formation of large aggregates in the presence of salt and can be attributed to the transformation of the small spherical vesicles to large vesicles or tube/rod-like aggregates. Since the surfactant solution at high salt concentration remained optically clear the possibility of formation of large vesicles can be ruled out. To visually observe the shape of larger

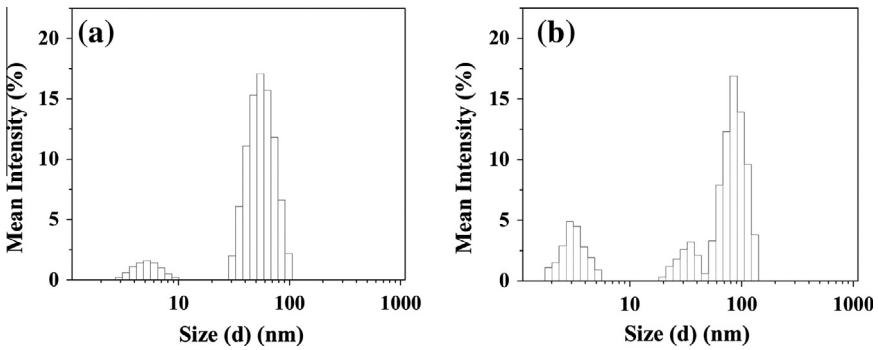

Fig. 4. Hydrodynamic size distributions of the surfactant aggregates in (a) 5 mM and (b) 20 mM aqueous C_{12}-CAR solutions at 298 K.

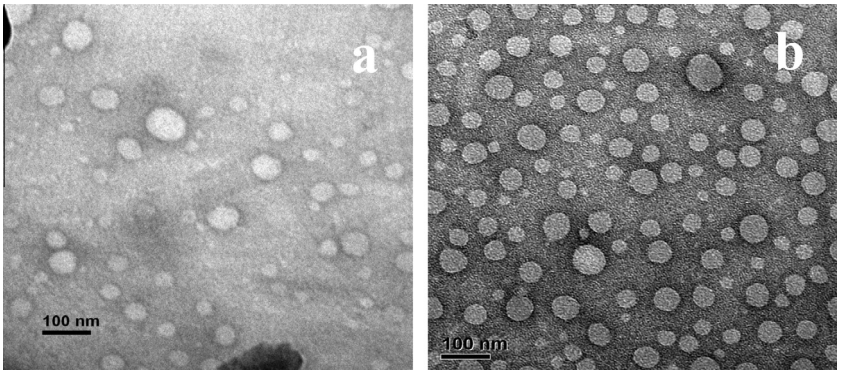

Fig. 5. TEM micrographs (negatively stained with 1% uranyl acetate) of (a) 5.0 mM and (b) 20.0 mM C_{12}-CAR.

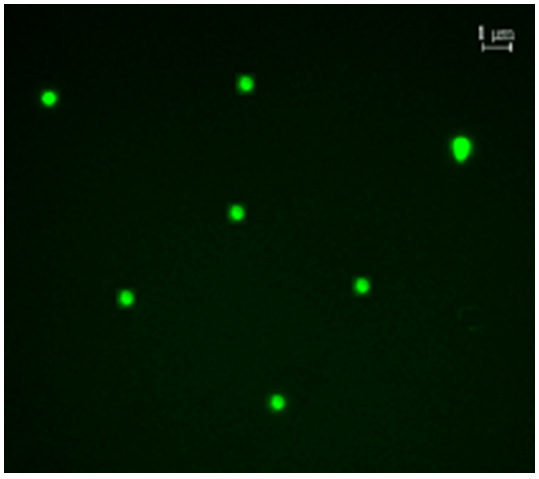

Fig. 6. Fluorescence microscopic image of CF-trapped vesicle solution of C_{12}-CAR.

aggregates we have measured TEM micrograph of the 5 mM C_{12}-CAR solution containing 50 mM NaCl. Clearly, the micrograph (Fig. 7(b)) reveals the presence of a bunch of long aggregates of tubular morphology. The tubules are not flexible. They are a few micrometers long and have an inner diameter around 50–100 nm. If they were flexible rod-like aggregates, the surfactant solution would be viscous. Since the diameter of the long aggregates is very large and surfactant solution did not appear viscous, they can be associated with tubular aggregates. Because there are no marks on the surface of the nanotubes, they are probably formed by rolling (like cigarette paper) of the bilayer sheets formed at higher surfactant concentrations. The existence of such morphology in C_{12}-CAR at high salt concentrations is thus consistent with the results of DLS and fluorescence measurements.

3.7. Effect of cholesterol on vesicle stability

Cholesterol (Chol) is an integral part of biological membranes and is known to influence the packing of lipids within the bilayer which in turn affects bilayer permeability, mechanical strength and biochemical interactions [44]. In general, co-lipids like Chol are required for transfection because it offers rigidity and stability to the liposomes. Also cell membrane has Chol receptors, which help in the fusion of liposomes on the cell surface. In order to evaluate the effect of Chol on the stability of bilayer membranes formed by C_{12}-CAR surfactant, we performed fluorescence anisotropy measurements using a DPH probe in the presence of varying concentrations of Chol. It was found that with increase in [Chol] in the lipid mixture with C_{12}-CAR the *r*-value increases reaching maximum at ca. 10 mol% of Chol (Fig. 8). Upon further addition of Chol the *r*-value decreased slightly and the physical appearance of the measuring solution becomes turbid. For C_{12}-CAR, the increase of *r*-value in the presence of Chol indicates that addition of Chol makes the bilayer membrane more rigid, which offers more stability to the vesicles. The Chol incorporation into the bilayer results in a greater head-group separation and thereby minimizes the electrostatic repulsions between the Me_3N^+ units at the level of head-groups of C_{12}-CAR monomers and offers an extra stability to the bilayer self-assembly [37]. At higher level (>10 mol%) of Chol, the *r*-value starts to fall indicating that the Chol has reached its solubility limit in lipid bilayers.

3.8. Thermal stability of vesicles

Determination of physical stability of vesicles at higher temperature is necessary for their practical applications and therefore, the effect of temperature on vesicular stability of C_{12}-CAR was also studied. The fluorescence anisotropy of DPH probe solubilized in

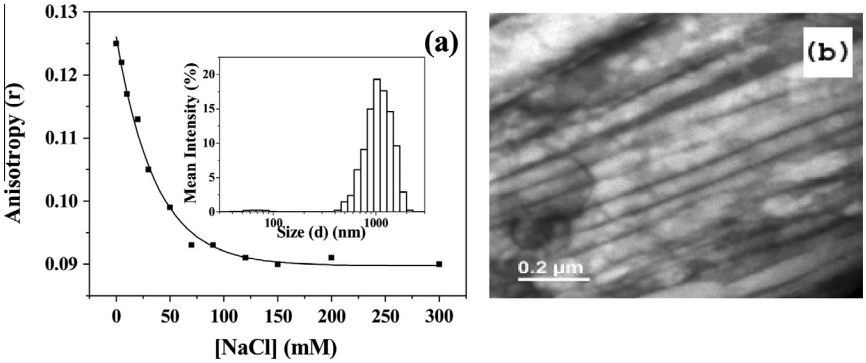

Fig. 7. (a) Plot of *r* of DPH vs [NaCl] in 5.0 mM C_{12}-CAR solution; Inset: Size distribution profile of 5.0 mM C_{12}-CAR aggregates in the presence of 50 mM NaCl at 298 K; (b) TEM micrographs (negatively stained with 1% uranyl acetate) of 5.0 mM C_{12}-CAR in the presence of 50 mM NaCl at 298 K.

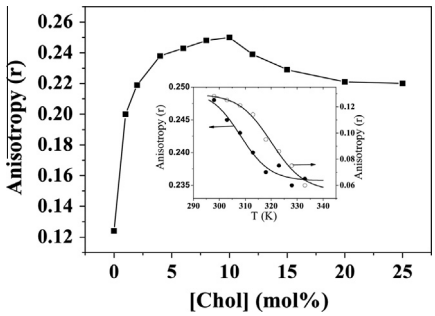

Fig. 8. Plot of r of DPH as a function of mol % of Chol in 5.0 mM C_{12}-CAR at 298 K; Inset: plots of r of DPH versus T (K) for 5.0 mM C_{12}-CAR without (○) and with 10 mol% Chol mixture (●).

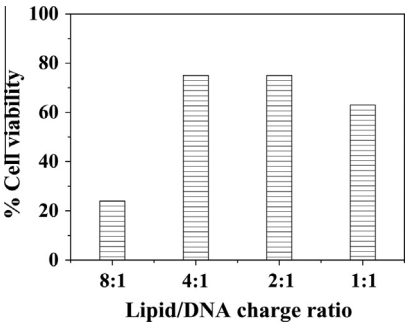

Fig. 10. Bar graphs of percent cell viability versus lipid-to-DNA (+/−) charge ratio for C_{12}-CAR liposome in CHO cells.

the vesicles bilayer was monitored in the temperature range 298–333 K. The plots in the inset of Fig. 8 show the variation of r with temperature in 5 mM aqueous C_{12}-CAR solution. The r-value which is higher at low temperatures decreases with the increase in temperature. This is because of the decrease of microviscosity of the vesicle bilayer with the rise of temperature as a result of weakening of the hydrophobic interactions among hydrocarbon chains as well as the disruption of the intermolecular H-bonding and other physical forces forming the bilayer aggregates. The sigmoid plot suggests a two-state transition. Since the r-value (0.06) detected at 333 K is very low and corresponds to micellar structure, the sigmoid decrease of r-value can be attributed to vesicle-to-micelle transition. Thus the temperature corresponding to a 50% change of r can be taken as melting or phase transition temperature, T_m of the vesicles. The high value of transition temperature (~315 K) clearly suggests that the vesicles are quite stable at physiological temperature (310 K).

Bhattacharya and Haldar observed that the hydrophobic association of the cationic amphiphile and Chol imposes restriction on the chain $(CH_2)_n$ motions, and offers rigidity to the self-assembly [37]. This modulation in the hydrocarbon chain fluidity in the lipid bilayer can in turn alter T_m value and thus enhance vesicle stability. We therefore measured the r-value of DPH in C_{12}-CAR/Chol mixture at different temperatures (Fig. 8 (inset)). A thermal phase transition as indicated by a small sigmoid decrease of r-value can be clearly seen. This can be attributed to gel-to-liquid crystal phase transition with T_m at around 311 K. The higher r-values at the elevated temperatures suggests that the packing of hydrocarbon chains of the bilayer formed by C_{12}-CAR/Chol lipid mixture is very rigid and that the vesicles are highly stable even at 333 K.

3.9. In vitro gene transfection study

Many cationic amphiphiles have been reported for safe and target specific delivery of genetic materials in gene therapy [7,45]. The gene transfection efficiency depends largely on the structure of the cationic amphiphile [45]. The double chain alkyl/acyl carnitine esters were reported [14] as potentially biodegradable cationic lipids for use in gene delivery. Keeping in mind the recent developments in non-viral vectors in gene transfection, a preliminary biocompatibility and gene delivery studies were carried out with C_{12}-CAR surfactant. The transfection efficiency of the liposome prepared from C_{12}-CAR-Chol mixture was compared with lipofectamine-2000, a commercially available liposome. The detailed procedure for liposome preparation, cell culture, and transfection assays is described under supporting information. For confirmation of gene transfection and its expression within the cells the β-galactosidase activity was assayed. All the transfection experiment was carried out in duplicate to ensure the reproducibility, and the transfection efficiency values shown in Fig. 9 for (a) CHO and (b) COS-1 cells are the average of triplicate experiments performed on the same day. Transfection efficiency of the liposome was compared with that of lipofectamine-2000. The gene transfection results suggest that the liposomes prepared from C_{12}-CAR and Chol in 5:1 mol ratio are able to transfect DNA into the cell. Gene transfection was found to be better in 2:1 and 4:1 lipid-to-DNA (+/−) charge ratios and a better result of transfection was obtained for liposome in COS-1 cells.

3.10. Cytotoxicity study

Cytotoxicity of the liposomes was assessed by the 3-(4,5-dimethyl-thiazol-2-yl)-2,5-diphenyltetrazolium bromide (MTT) reduction assay in CHO cells [46]. The cytotoxicity assay was performed in 96-well plates by maintaining the same ratio of number of cells to amount of cationic lipid, as used in the transfection experiments. 10 μL of MTT solution (5 mg MTT/mL in PBS) was added 4 h after addition of cationic lipid to the cells. The cell plate is kept for 4 h in the incubator and the violet crystal was

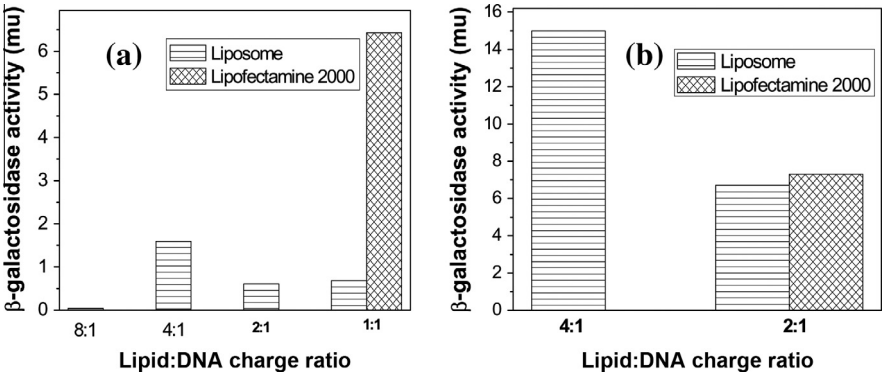

Fig. 9. In vitro gene transfection efficiencies of C_{12}-CAR-Chol liposomes into (a) CHO cells; and (b) COS-1 cells.

observed on the cell plate in which MTT was added. Methanol/DMSO mixture (1:1, v/v) was added to dissolve the crystal and shaken for 10 min. Finally, absorbance value at 550 nm was measured in a model ELx- 800Ms spectrophotometer. Results were expressed as percent viability (=[A_{540}(treated cells) – background/A_{540} (untreated cells) – background] × 100) and are summarized in Fig. 10. The cytotoxicity results suggest that the cells are more viable in the presence of liposome-DNA complex having 2:1 and 4:1 lipid-to-DNA (+/−) charge ratios. However, at 8:1 lipid-to-DNA (+/−) charge ratio, the cells are found to be least viable. This might be the reason for better gene transfection efficiencies of the liposome-DNA complexes of 2:1 and 4:1 lipid-to-DNA (+/−) charge ratios.

4. Conclusions

In summary, a new single-chain, biocompatible cationic surfactant, (3-dodecylcarbamoyl-2-hydroxypropyl)trimethylammonium chloride, C_{12}-CAR, was synthesized. The interfacial properties and self-assembly behavior of C_{12}-CAR were investigated in aqueous medium. The low *cac* and γ_{cac} values depict the amphiphile as a reasonably good surface-active agent. Unlike structurally similar conventional single-chain cationic surfactants [29,33] and most of the single-chain acyl carnitine derivatives (zwitterionic surfactants) [18,19] which form micelles at low concentrations, C_{12}-CAR was found to self-organize spontaneously to form stable vesicles in aqueous solution in a wide range of concentrations. The size of the vesicles ranges between 30 nm and 70 nm. The presence of the —OH and HNC═O groups in the hydrocarbon chain of C_{12}-CAR promotes the bilayer aggregate formation through intermolecular H-bonding interactions between the surfactant monomers. The results of microviscosity (η_m) and anisotropy (r) measurements suggest that the vesicle phase of the amphiphile is quite stable. However in the presence of NaCl at concentrations greater than 50 mM, the vesicles slowly transform into rigid elongated tubular aggregates. The results of fluorescence probe studies indicate the rigid bilayer vesicle membrane is capable of solubilizing nonpolar molecules. On the other hand, fluorescence microscopy confirmed entrapment of polar molecules in the aqueous core of vesicles. It was observed that vesicles formed by C_{12}-CAR/Chol mixture have more rigid bilayer membrane, which offers an extra stability to the vesicle structure even at high temperatures (>310 K). Liposomes obtained from the C_{12}-CAR/Chol mixture were found to be nontoxic and could deliver plasmid DNA into both CHO and COS-1 cells. The gene transfection efficiency of the cationic surfactant was found to be comparable to the commercially available standard lipofectamine-2000. Since the C_{12}-CAR/Chol/DNA complexes are nontoxic, the C_{12}-CAR/Chol mixture can have potential application in gene delivery. Thus, as far as gene delivery is concerned, the single-chain carnitine amide amphiphile is as good as the double chain alkyl/acyl carnitine esters [14].

Acknowledgments

The authors gratefully acknowledge the Department of Science and Technology, New Delhi for financial support (Grant No. SR/S1/PC-18/2005) of this work. We thank Dr. Arabinda Chaudhuri, IICT Hyderabad for assistance with the gene transfection measurements, Prof. Nilmoni Sarkar, IIT Kharagpur for DLS measurements and Prof. N. Chattopadhyay, Jadavpur University, Kolkata, for assistance with the fluorescence lifetime measurements.

Appendix A. Supplementary material

Supplementary data associated with this article can be found, in the online version, at http://dx.doi.org/10.1016/j.jcis.2014.08.049.

References

[1] J.H. Felgner, R. Kumar, C.N. Sridhar, C.J. Wheeler, Y.J. Tsai, R. Border, P. Ramsey, M. Martin, P.L. Felgner, J. Biol. Chem. 269 (1994) 2550–2561.
[2] M.T.N. Campanhã, E.M. Mamizuka, A.M. Carmona-Ribeiro, Lipid Res. 40 (1999) 1495–1500.
[3] R.R.C. New, M.L. Chance, S.C. Thomas, W. Peters, Nature (London) 272 (1978) 55–56.
[4] G. Lopez-Berestein, G.P. Bodey, L.S. Frankel, K. Mehta, J. Clin. Oncol. 5 (1987) 310–317.
[5] D.B. Vieira, A.M. Carmona-Ribeiro, J. Antimicrob. Chemother. 58 (2006) 760–767.
[6] A.A. Kadry, S.A. Al-Suwayeh, A.R.A. Abd-Allah, M.A. Bayomi, J. Antimicrob. Chemother. 54 (2004) 1103–1108.
[7] R. Srinivas, S. Samanta, A. Chaudhuri, Chem. Soc. Rev. 38 (2009) 3326–3338.
[8] P.C.A. Barreleiro, R.P. May, B. Lindman, Faraday Discuss. 122 (2003) 191–201.
[9] Y. Xu, F.C. Szoka Jr., Biochemistry 35 (1996) 5616–5623.
[10] D. Llères, J.P. Clamme, E. Dauty, T. Blessing, G. Krishnamoorthy, G. Duportail, Y. Mély, Langmuir 18 (2002) 10340–10347.
[11] P. Pinnaduwage, L. Schmitt, L. Huang, Biochim. Biophys. Acta 985 (1989) 33–37.
[12] B. Kamm, M. Kamm, A. Kiener, H.P. Meyer, Appl. Microbiol. Biotechnol. 67 (2005) 1–7.
[13] J. Cervenka, H. Osmundsen, J. Lipid. Res. 23 (1982) 1243–1246.
[14] J. Wang, X. Guo, Y. Xu, L. Barron, F.C. Szoka, J. Med. Chem. 41 (1998) 2207–2215.
[15] M. Calvani, L. Critelli, G. Gallo, F. Giorgi, G. Gramiccioli, M. Santaniello, N. Scafetta, M.O. Tinti, F. De Angelis, J. Med. Chem. 41 (1998) 2227–2233.
[16] J.B. Nivet, M.L. Blanc, J.G. Riess, Eur. J. Med. Chem. 26 (1991) 953–960.
[17] N. Bodor, J.J. Kaminsky, S. Selk, J. Med. Chem. 23 (1980) 469–474.
[18] S.H. Yalkowsky, G. Zografi, J. Colloid Interf. Sci. 34 (1970) 525–533.
[19] M. Cipollone, P. De Maria, A. Fontana, S. Frascari, L. Gobbi, D. Spinelli, M. Tinti, Eur. J. Med. Chem. 35 (2000) 903–911.
[20] P. Stano, S. Bufali, C. Pisano, F. Bucci, M. Barbarino, M. Santaniello, P. Carminati, P.L. Luisi, J. Liposome Res. 14 (2004) 87–109.
[21] T. Tomohiro, Y. Ogawa, H. Okuno, M. Kodaka, J. Am. Chem. Soc. 125 (2003) 14733–14740.
[22] M.J. Rosen, Surfactants and Interfacial Phenomena, fourth ed., Wiley-Interscience, New York, 2004.
[23] J. Eastoe, S. Nave, A. Downer, A. Paul, A. Rankin, Langmuir 16 (2000) 4511–4518. and references therein.
[24] S. Roy, D. Khatua, J. Dey, J. Colloid Interf. Sci. 292 (2005) 255–264.
[25] A. Ghosh, J. Dey, Langmuir 24 (2008) 6018–6026.
[26] J. Sawayama, I. Yoshikawa, K. Araki, Langmuir 26 (2010) 8030–8035.
[27] J.R. Lakowicz, Principles of Fluorescence Spectroscopy, Plenum Press, New York, 1983. pp. 132.
[28] K. Kalyanasundaram, J.K. Thomas, J. Am. Chem. Soc. 99 (1977) 2039–2044.
[29] S.P. Moulik, M.E. Haque, P.K. Jana, A.R. Das, J. Phys. Chem. 100 (1996) 701–708.
[30] T. Saitoh, K. Taguchi, M. Hiraide, Anal. Chim. Acta. 454 (2002) 203–208.
[31] H. Saito, K. Nishiwaki, T. Handa, S. Ito, K. Miyajima, Langmuir 11 (1995) 3742–3747.
[32] U. Cogan, M. Shinitzky, G. Weber, T. Nishida, Biochemistry 12 (1973) 521–528.
[33] S. Roy, A. Mohanty, J. Dey, Chem. Phys. Lett. 414 (2005) 23–27.
[34] M. Manconi, R. Isola, A.M. Falchi, C. Sinico, A.M. Fadda, Colloids Surf. B, Biointerf. 57 (2007) 143–151.
[35] W. Al-Soufi, L. Piñeiro, M. Novo, J. Colloid Interf. Sci. 370 (2012) 102–110.
[36] B.V. Shankar, A. Patanaik, Langmuir 23 (2007) 3523–3529.
[37] S. Bhattacharya, S. Haldar, Biochim. Biophys. Acta, Biomembr. 1283 (1996) 21–30.
[38] M. Popov, C. Linder, R.J. Deckelbaum, S. Grinberg, I.H. Hansen, E. Shaubi, T. Waner, E. Heldman, J. Liposome Res. 20 (2010) 147–159.
[39] F. Reiss-Husson, V. Luzzati, J. Phys. Chem. 68 (1964) 3504–3511.
[40] A. Mohanty, T. Patra, J. Dey, J. Phys. Chem. B 111 (2007) 7155–7159.
[41] X. Wang, J. Zhu, J. Wang, G. Zeng, J. Dispersion Sci. Technol. 29 (2008) 83–88.
[42] Y. Yan, W. Xiong, X. Li, T. Lu, J. Huang, Z. Li, H. Fu, J. Phys. Chem. B 111 (2007) 2225–2230.
[43] S.J. Ryhänen, V.M.J. Säily, M.J. Parry, P. Luciani, G. Mancini, J.M.I. Alakoskela, P.K.J. Kinnunen, J. Am. Chem. Soc. 128 (2006) 8659–8663.
[44] F.R. Maxfield, G. van Meer, Curr. Opin. Cell Biol. 22 (2010) 422–429.
[45] X. Guo, L. Huang, Acc. Chem. Res. 45 (2012) 971–979.
[46] C. Aiello, P. Andreozzi, C. La Mesab, G. Risuleo, Colloids Surf. B: Biointerf. 78 (2010) 149–154.